
# Nutritional deficiency and placenta calcification underlie constitutive, selective embryo loss in pregnant South American plains vizcacha, *Lagostomus maximus* (Rodentia, Caviomorpha)

Mariela Giacchino, Juan A. Claver, Pablo IF. Inserra, Fernando D. Lange, María C. Gariboldi, Sergio R. Ferraris, Alfredo D. Vitullo

PII: S0093-691X(20)30353-8

DOI: https://doi.org/10.1016/j.theriogenology.2020.06.003

Reference: THE 15559

To appear in: *Theriogenology*

Received Date: 11 December 2019

Revised Date: 25 May 2020

Accepted Date: 4 June 2020

Please cite this article as: Giacchino M, Claver JA, Inserra PI, Lange FD, Gariboldi MaríC, Ferraris SR, Vitullo AD, Nutritional deficiency and placenta calcification underlie constitutive, selective embryo loss in pregnant South American plains vizcacha, *Lagostomus maximus* (Rodentia, Caviomorpha), *Theriogenology* (2020), doi: https://doi.org/10.1016/j.theriogenology.2020.06.003.

Credit Author Statement

*Conceptualization:* Mariela Giacchino and Alfredo D. Vitullo

*Formal analysis:* Mariela Giacchino, Juan A. Claver, Pablo I. F. Inserra and Alfredo D. Vitullo

*Funding acquisition:* Sergio R. Ferraris and Alfredo D. Vitullo

*Investigation:* Mariela Giacchino, Juan A. Claver, Pablo I. F. Inserra, Fernando D. Lange, María C. Gariboldi and Sergio R. Ferraris

*Methodology:* Mariela Giacchino, Juan A. Claver, Pablo I. F. Inserra, Ferandno D. Lange, María C. Gariboldi, Sergio R. Ferraris and Alfredo D. Vitullo

*Project administration:* Mariela Giacchino and Alfredo D. Vitullo

*Resources:* Mariela Giacchino, Juan A. Claver, Pablo I. F. Inserra, Fernado D. Lange, María C. Gariboldi, Sergio R. Ferraris and Alfredo D. Vitullo

*Supervision:* Alfredo D. Vitullo

*Validation:* Mariela Giacchino, Juan A. Claver and Pablo I. F. Inserra

*Visualization:* Mariela Giacchino and Pablo I. F. Inserra

*Writing - original draft preparation:* Mariela Giacchino, Pablo I. F. Inserra, María C. Gariboldi and Alfredo D. Vitullo

*Writing - review & editing:* Mariela Giacchino, Juan A. Claver, Pablo I. F. Inserra, María C. Gariboldi and Alfredo D. Vitullo

**REVISED**

# Nutritional deficiency and placenta calcification underlie constitutive, selective embryo loss in pregnant South American plains vizcacha, *Lagostomus maximus* (Rodentia, Caviomorpha)

Mariela Giacchino[1,2], Juan A Claver[3], Pablo IF Inserra[1,2], Fernando D Lange[4], María C Gariboldi[1,2], Sergio R Ferraris[4] & Alfredo D Vitullo[1,2,*]

[1]Centro de Estudios Biomédicos Básicos, Aplicados y Desarrollo (CEBBAD)[§], Universidad Maimónides, Buenos Aires, Argentina.

[2]Consejo Nacional de Investigaciones Científicas y Técnicas (CONICET), Argentina.

[3]Cátedra de Histología y Embriología, Facultad de Ciencias Veterinarias, Universidad de Buenos Aires, Buenos Aires, Argentina.

[4]Centro de Ciencias Veterinarias (CCV)[¶], Universidad Maimónides, Buenos Aires, Argentina.

***Corresponding author:** Alfredo Daniel Vitullo. Phone: +54 11 4905-1100 ext. 1112. E-mail: vitullo.alfredo@maimonides.edu

[§]Formerly, Centro de Estudios Biomédicos, Biotecnológicos, Ambientales y Diagnóstico (CEBBAD) - Universidad Maimónides

[¶]Formerly, Centro de Investigación y Docencia en Medicina Experimental (CIDME) - Universidad Maimónides.

**Running head:** Selective embryo loss in *Lagostomus maximus*.

**Abstract**

Plains vizcacha females are able to ovulate up to 800 oocytes per estrus cycle. However, just 10-12 embryos are implanted and only two of them, those located nearest the cervix, are gestated to term. Between 26 and 70 days post-coitum, a constitutive resorption occurs from the embryos located proximal to the ovary, extending progressively toward those distally implanted. Our previous studies on the dynamics of gestation in *L. maximus*, led us to hypothesize some kind of placental and nutritional insufficiency as the basis for the resorption process. We analyzed histology and arterial architecture of the reproductive tract in pregnant and non-pregnant females. Uterine horns are irrigated through the uterine artery, a branch of the internal iliac artery, in an ascending way from the cervix; segmental arteries irrigating the embryo vesicles become thinner as they approach the ovary. Contrast solution administered during angiographies accumulated in the placenta of embryos closest to cervix. Thus, blood stream favors the embryos nearest the cervix, indicating a gradual nutritional deficiency of those closest to the ovary. Besides, placenta becomes calcified early, at mid-gestation, during the resorption process. Finally, the detection of specialized endothelial venules and inflammatory cells suggest the concurrent participation of immunological processes in embryo vesicles undergoing resorption.

**Keywords:** Vizcacha, Uterine circulation, Embryo resorption, Placenta calcification, Nutritional deficiency, Pseudoseptum.

## Introduction

The South American plains vizcacha, *Lagostomus maximus*, is a hystricomorph rodent distributed from the Pampas of Argentina to the southern areas of Bolivia and Paraguay [1-4]. Females display several unusual reproductive traits, including the highest ovulation rate recorded among mammals and a process of selective embryonic resorption that occurs during the first half of a 155-day long gestation [5]. Although ovulation can reach up to 800 oocytes at each estrus cycle, a small proportion of eggs are fertilized and a few 8 to 12 embryos are successfully implanted, distributed in each uterine horn, following an 18-day long preimplantation period [6]. Soon after implantation, between 26 and 70 days post-coitum (dpc), resorption takes place from the embryos located proximal to the ovary extending progressively toward those distally implanted [7]. At the end of the resorption process, only the embryos implanted nearest the cervix are still surviving and develop to term [6]. This process of partial embryonic resorption that results in the delivery of only two pups occurs in each pregnancy as a constitutive event that characterizes the species. Once resorption has been completed, from 70dpc onwards an ovulation-like event occurs, promoted by the activation of the hypothalamic-hypophyseal-gonadal axis, following a decrease in circulating progesterone [8]. As a result, a considerable number of accessory corpora lutea are added [9]. We have previously hypothesized that the addition of newly developed corpora lutea at mid-gestation could help to recover progesterone levels and rescue the only two surviving, distally implanted fetuses that escaped resorption [9]. In support, we showed that the decrease of progesterone level from mid-gestation enables follicular recruitment until pre-ovulatory stage and the development of functional accessory corpora lutea which help to recover progressively the level of progesterone [10]. Furthermore, the decrease in progesterone level at mid-gestation was suspected to arise from some kind of placental insufficiency [9].

Considering the constitutive and selective nature of embryonic resorption in *L. maximus*, we focused on nutritional deficiency and uterine and placental alterations as possible causes of embryo loss. Regarding a possible nutritional deficiency; we analyzed the arterial architecture and blood supply of the reproductive tract, with special emphasis in pregnant females. We also investigated the anatomy and histology of the uterine horns throughout the reproductive cycle and the general histology of the placenta in order to find clues that might help to explain or understand the resorption process.

## Materials and methods

### Ethics

All experimental protocols concerning animals were conducted in accordance with the guide for the care and use of laboratory animals published by the National Research Council [11], and were reviewed and approved by the Institutional Committee of Use and Care of Laboratory Animals (CICUAL; Res. 2014/5) from Facultad de Ciencias Veterinarias, Universidad de Buenos Aires, and the Institutional Committee on Use and Care of Experimental Animals (CICUAE) from Universidad Maimónides, Argentina. Appropriate procedures were performed to minimize the number of animals used. Capture, handling and transportation of animals were approved by Buenos Aires Province Government Authority, Dirección de Flora y Fauna, Ministerio de Agroindustria.

**Animals**

Adult female plains vizcachas (n=70) -2.5 to 3.0kg body weight; 2-2.5 years old determined by the dry crystalline lens weight according to Jackson [12]- were captured from a resident natural population at the Estación de Cría de Animales Silvestres (ECAS), Villa Elisa, Buenos Aires Province, Argentina, using live-traps located at the entrance of burrows. In order to obtain females at different reproductive stages, captures were planned according to the natural reproductive cycle which extends from February to August as described by Llanos & Crespo [1], and our own field expertise [8-10; 13-18]. Non-gestating adult females (n=17) were captured in early February, when reproductive season starts. Early-pregnant females (n=16) were captured in April, mid-pregnant females (n=16) in July and late-pregnant females (n=14) in August. Gestational age was estimated on the basis of the capture time and fetal development, according to Leopardo *et al*. [14]. Post-partum, lactating adult females (n=7) were captured from August to September. Pre-pubertal females (n=5), born in captivity in August, were kept with their mothers for 30 days until weaning before used.

**Angiography of the reproductive tract of the female vizcacha**

To determine the blood supply of the reproductive tract, non-pregnant (n=6), early-pregnant (n=4) and mid-pregnant (n=4) females were anesthetized by intramuscular injection of 10mg/kg body weight ketamine chlorydrate (Holliday Scott S.A., Buenos Aires, Argentina) and 1mg/kg body weight xylazine chlorhydrate (Richmond Laboratories, Buenos Aires, Argentina). To prevent arterial thromboembolism, animals were administered an intramuscular injection of 400-600IU/kg of heparin. After shaving the abdomen, females were positioned lying on their backs (supine position) on a digital mobile C-arm X-ray system with fluoroscopy and an image enhancer (Toshiba, 125kv and 500mA) and the abdominal cavities were exposed. A contrast solution (Triyosom®, amidotrizoic acid, Berlimed, Madrid, Spain) was injected at 3 different sites into the abdominal aorta; upper descending aorta, at the level of renal artery branch and

1cm above the iliac arteries branches (Fig. 1). Images were taken as print captures at different moments during the angiographic procedure.

**Vascular casting of the reproductive tract of the female vizcacha with latex**

After the angiographies, females were sacrificed by trained veterinary staff with an intracardiac injection of 0.5 ml/kg body weight of Euthanyl (0.5ml/kg body weight, sodium pentobarbital, sodium diphenylhydantoin, Brouwer S. A., Buenos Aires, Argentina). Four animals at term-pregnancy were incorporated to the study at this point. Vascular lavage was performed by the intraventricular administration of 150ml of physiological solution. Vascular casting was performed according to Rezende *et al* . [19]. Briefly, 40ml of red latex were injected through the abdominal aorta, 1cm above the iliac branches, to shape the vascular architecture of the female reproductive tract (Fig. 1). Corpses were rested for 2h at room temperature and then fixed in 10% formaldehyde for 48h. Chemical tissue digestion was performed by incubating the bodies with 50% sodium hypochlorite solution for 24h. Mechanical digestion was performed to remove the remaining tissue. Representative images were taken using a stereoscopic microscope (Nikon C-DSD230, Tokyo, Japan), fitted with a digital camera (390CU 3.2 Megapixel CCD Camera, Micrometrics, Spain) and the image software Micrometrics SE P4 (Standard Edition Premium 4, Micrometrics, Spain).

**Tissue samples**

Non-pregnant (n=11), early-pregnant (n=12), mid-pregnant (n=12), late-pregnant (n=10), lactating adult females (n=7) and pre-pubertal females (n=5) were anesthetized and sacrificed as described above. Uterine horns were immediately removed and processed for optical or electron microscopy (see below). The uterine horns of pregnant females were exposed and the fetuses were immediately removed with their placentas and fixed for further analysis.

**Optical microscopy**

Tissue samples (n=52) were fixed in 10% formaldehyde for 24h, dehydrated through a graded series of ethanol (70, 96 and 100%) and embedded in paraffin. Samples were entirely cut in 5µm-thick serial sections and mounted onto cleaned coated slides. Sections were dewaxed in xylene and rehydrated through a decreasing series of ethanol. Selected sections of each specimen were used for classical hematoxylin and eosin (H&E) and Masson's trichrome stain for general description. Horns of lactating females (n=7) were stained with Prussian blue, and mid- (n=12) and late-gestating placentas (n=10) with Von Kossa staining for specific description. Representative images were captured with an optic microscope (BX40, Olympus Optical Corporation, Tokyo, Japan), fitted with a digital camera (390CU 3.2 Megapixel CCD

Camera, Micrometrics, Spain, and the image software Micrometrics SE P4 (Standard Edition Premium 4, Micrometrics, Spain).

**Transmission electron microscopy**

Oviduct samples from non-pregnant adult females (n=5) were initially fixed in 3% glutaraldehyde in 0.1M phosphate buffer (PBS) for 24h and then transferred to fresh PBS for 48h. A second round of fixation was performed with 1% $OsO_4$ for 60min at 0ºC. Samples were washed twice with distilled water for 15min. A final round of fixation was performed incubating samples overnight with 5% uranyl acetate followed by two 15-min washings with distilled water. Samples were then dehydrated through a graded series of ethanol followed by two 10-min immersions in acetone. Samples were embedded in Durcupan resin and polymerized at 60ºC for 72h. Ultrathin sections (50nm thick) were cut by an ultramicrotome (Reichert Jung Ultracut E, Wien, Austria). Finally, sections were mounted on copper grids and counterstained with 5% uranyl acetate and 2.5% lead citrate. Representative images were captured with a Zeiss EM 109T transmission electron microscope (Zeiss, Oberkochen, Germany).

**Analysis of placental apoptosis by TUNEL assay**

Apoptosis-associated DNA fragmentation was detected in mid- (n=5) and late-pregnant (n=5) placenta by the TUNEL technique [20] using the *in situ* Cell Death Detection Kit (Roche Diagnostics, Roche Applied Science), as previously described in vizcacha [9, 13-15]. Mounted sections were dewaxed in xylene, rehydrated through a decreasing series of ethanol (100, 96, 80, 70 and 50%) and PBS, and permeabilized with 20 µg/ml nuclease-free proteinase K in 10 mM Tris-HCl (Invitrogen, Life Technologies Corporation) for 20 min at 37 °C. The TUNEL reaction was carried out following the supplier's recommendations. The sections were incubated with the TUNEL reaction mixture (labelling solution plus the terminal transferase enzyme) for 60 min at 37 °C. Sections were mounted with DAPI (Vectashield, Vector laboratories, California, USA) and coverslipped. A negative control assay was carried out by omitting the terminal transferase enzyme. Reaction was visualized with a laser microscope (Nikon C1 Plus Inverted Research Microscope Eclipse Ti, Nikon Corporation., Tokyo, Japan) and fitted with the image software EZ-C1 (Software v3.9, Nikon Ltd. London, UK). Representative images were taken.

**Results**

**Circulation of the reproductive tract of the female vizcacha**

The angiography of non-pregnant adult females showed no evidence of the uterine arteries when the contrast solution was administered to the abdominal aorta (Fig. 2A) or the renal arteries (not

shown). However, uterine arteries were visualized when the contrast solution was injected above the iliac artery bifurcation (Fig. 2B). Each uterine artery showed an ascending trajectory, with arterial branches, segmental arteries, toward the uterine horn (Fig. 2B). The administration of the contrast solution to the iliac artery bifurcation in early-pregnant females revealed all the embryonic vesicles implanted in the uterine horns (Fig. 2C-D). An increment in the blood vessels caliber was evident at this stage. Regardless of the volume of the contrast solution administered, the analysis of the perfusion along the entire uterine horn in mid-pregnant females was not possible since all the contrast solution accumulated in the placental vessels of the first embryonic vesicle (E1), implanted nearest the cervix (Fig. 2E-F). Hence, the procedure was not performed in more advanced gestational stages.

The vascular latex cast of the reproductive tract of the female vizcacha displayed a detailed view of the uterine circulation (Fig. 3). The artery that irrigates each uterine horn is a branch of the internal iliac arteries originating 1.5 cm after the bifurcation of the abdominal aorta. The uterine artery is located medially at the iliac crests, dorsal to the bladder and follows an ascending path through the broad ligament of the uterus (Fig. 3A-B). The uterine artery emits segmental branches that irrigate the vagina, cervix, uterine horns and pseudosepta (Fig. 3C). In early pregnant females, segmental branches of the uterine artery displayed a larger caliber at E1, where the surviving embryo is implanted, compared to the caliber of segmental branches irrigating the embryonic vesicles that are being resorbed (Fig. 3D-E). Additionally, uterine horns at mid-pregnancy presented a septum that separated the surviving fetus from the embryonic resorption remains (Fig. 3F). At the distal end, the uterine arteries anastomose to the ovarian arteries (Fig. 3G-H). Figure 4 shows a schematic representation of the vascular circulation of the genital tract.

**Macroscopic and histological analysis of the reproductive tract of the female vizcacha**

The uterine horns of pre-pubertal females showed three underdeveloped layers: endometrial (simple cylindrical epithelium and a lamina propria with short tubular glands), muscular (longitudinal external layer, a badly defined mid layer and a circular inner layer) and serosa (Fig. 5A). The vagina presented a pseudostratified epithelium with mucous cells (Fig 5B), while the endometrium showed a cylindrical simple epithelium, with loose stroma and scarce endometrial glands (Fig 5C).

Macroscopically, the uterine horns of non-pregnant adult females presented muscular development with a longitudinal banding shape (Fig. 6A). Inside the vagina, the bifurcation of both uterine horns was determined by a vaginal septum in the anterior region of the organ (Fig. 6B). Female vizcacha lacks a defined cervix. It appears to be continuity between the vagina and

the uterine horn characterized by a fold of the mucosa and a poor muscular development (Fig. 6B). Longitudinal sections of the horn showed a zigzag pattern of the uterine cavity (Fig. 6C). No transition between the vaginal and the uterine epithelium was observed. The stratified epithelium with a superficial layer of mucous cells of the vagina changed abruptly into a simple cylindrical epithelium in the uterus (Fig. 6D). The vagina presented high endothelium venules (HEV) with simple cubical epithelium (Fig. 6E). The oviduct cavity showed partitions that produced separated compartments (Fig. 6F). In the ampulla, peg cells presented nuclei protrusion and cytoplasm prolongations towards the cavity (Fig. 6G). Transmission electron microscopy revealed ciliated and secretory cells in the oviduct epithelium (Fig. 6H). The cytoplasm of the secretory cells presented abundant secretory granules. The secreting product seems to be released together with part of the apical cytoplasm (Fig. 6I).

Early-pregnant females showed embryonic vesicles (E) of different size and color (Fig. 7A). E1 was the largest vesicle, nearest the cervix, and displayed a whitish color (Fig. 7B) while the remaining ones were smaller and darker (Fig. 7A). The smaller embryonic vesicles were necrotic and appeared as a hooked-sphere (Fig. 7C-D) due to the presence of pseudosepta between the embryos, with a small gap that communicates adjacent vesicles (Fig. 7E). Embryonic vesicles proximal to the ovary showed an advanced stage of resorption compared to those more distally located. E1 (nearest to the cervix) was the only vesicle with normal embryonic and extraembryonic structures (Fig. 8A-C). On the other hand, the vesicles being resorbed presented histological alterations in their organization (Fig. 8D). The second embryonic vesicle (E2) showed embryonic tissue invaded by inflammatory cells and remains of the yolk sac (Fig. 8E); the third embryonic vesicle (E3) presented only a central focus of fibrinoid necrotic material (Fig. 8F). The sections of the uterine horn where the necrotic vesicles were implanted showed prolongations that narrowed the space between vesicles. These prolongations consisted of connective tissue full of blood vessels (Fig. 8F). The endometrium presented ripples of the uterine surface in the area where the embryos were resorbed (Fig. 8G-H). Advanced stages of resorption displayed endometrial flaps between necrotic remains (Fig. 8I).

The uterine horns of lactating females showed extravasation of red blood cells in the endometrium. Multiple focuses of hemorrhage were registered, especially on the antimesometrial side of the endometrium (Fig. 9A) that developed in hemosiderosis. The endometrial stroma showed signs of reorganization, poor gland secretion and macrophages arranged in stipples (Fig. 9B). Iron granules, free or into macrophages were confirmed by Prussian blue stain (Fig. 9C).

**Histology of the placenta**

At mid-pregnancy, placenta of E1 showed calcium deposits in the basal decidua, and especially above the subplacenta (Fig. 10A, B). Calcium deposits were confirmed as black dots evidenced by von Kossa staining (not shown). TUNEL assay confirmed the presence of apoptotic cells in the subplacenta and in the basal decidua of E1 placenta of mid-pregnant females (Fig. 10C) whereas in advanced pregnancies apoptotic cells were only detected in the subplacenta (Fig. 10D). No positive apoptotic cells were detected in the labyrinth at any stage analyzed.

## Discussion

The anatomy and histology of the female reproductive tract of the vizcacha is, in general, comparable to that described for other hystricomorph rodents such as the coypu (*Myocastor coypus*) [21], the chinchilla (*Chinchilla lanigera*) [22], the green acouchi (*Myoprocta pratti*) [23] and the agouti (*Dasyprocta aguti*) [24]. Although our analysis is mostly consistent with previous descriptions of the female reproductive tract of *L. maximus* [6,7,17,25,26], a detailed inspection, especially throughout pregnancy, allowed us to detect novel characters not described so far, relate them to the circulatory system of the female genital tract and open new avenues for further investigation of the embryo resorption process that characterizes the species.

**Circulation of the female reproductive tract**

The uterine artery, arising from the internal iliac artery, irrigates the uterus as described in the chinchilla [22], the capybara (*Hydrochoerus hydrochaeris)* [27] and the guinea pig [28]. Angiographies revealed an ascending uterine circulation from the cervix toward the proximity of the ovary, with the areas of the uterine horns closest to the cervix being the first ones to be irrigated. In its ascending way, there is anastomosis of the uterine artery with the ovarian artery as it occurs in other caviomorph rodents and has also been recently reported in the vizcacha [29].

The ascending circulation pattern suggests that embryos implanted nearest the cervix benefit from receiving oxygen-, nutrient- and hormone-rich blood. In contrast, embryos implanted closer to the ovary, that will be resorbed, are irrigated by segmental branches born at more distal positions from the uterine artery. Moreover, the caliber of segmental branch arteries irrigating the embryos implanted nearest the cervix is wider than those irrigating embryos implanted more distally to the cervix. Angiographies performed in mid-pregnant females revealed that contrast solution accumulated in the placenta of embryos closest to cervix, despite the dose of contrast solution administered, indicating that those embryos are benefited with the greatest amount of the blood stream. The number and thickness of blood vessels also varied among the different

reproductive stages suggesting that steroid hormones play a central role in the vascular organization of the genital tract as reported in other studies [27, 30].

**General organization and novel histological traits of the reproductive tract**

Female vizcachas lack a defined cervix as described in the accouchi [23]. The transition between the vagina and the uterine horns is characterized by mucosa folding and a poor muscle development. The finding of high endothelial venules (HEV) in the vagina represents a novelty for the species. HEV are characteristic of lymphoid tissues and its presence in the reproductive tract is unusual [31]. HEV can develop from a normal epithelium at sites of chronic inflammatory processes facilitating the access of specific T cells [31]. The detection of this specialized endothelium suggests a possible relationship with the process of embryonic resorption enabling a direct access for lymphocytes, which deserves further investigation.

The oviduct and the uterine horns showed differentiated compartments. In the oviduct, the presence of trabecular structures created separate units of the lumen, comparable to those described in the mare [32]. These oviduct compartments, although not yet proved, have been associated to sperm storage [33]. In the ampullae, the epithelium showed cellular protrusions with detachment of cytoplasmic fragments and cellular loss as also described in the mare [32, 34]. It is not known, however, if this represents a physiological renewal of the epithelium, an apoptotic process or an apocrine secretion process as suggested by Steffl *et al.* [34]. Despite the function remains to be determined, the presence of those cells in the oviduct epithelium of the vizcacha is a constitutive character.

We have previously reported, by means of endoscopic inspection, incomplete partitions around the embryonic vesicles in the uterine horns of early pregnant females [17]. Histological analysis revealed that they are originated by transverse folds of the endometrial layer that grow toward the center, producing a partial obstruction of the uterine lumen. The growth of the endometrial mucosa constitutes a physical barrier between contiguous embryos that could contribute to the formation of differential environments. These changes of the endometrial mucosa could be related to the hormonal changes that take place throughout pregnancy. Although the communication between adjacent embryos is minimal, the separation between them is not complete, leaving a small opening in the center. This was revealed by the presence of remains of the resorbed embryos, probably generated by the protrusion of tissue through the center of the pseudoseptum. The separation of each embryonic vesicle could contribute to prevent that apoptotic and necrotic processes suffered in the embryonic vesicles implanted nearest the ovary spread to the embryos closest to the cervix, which are the only ones that will be gestated to term.

The embryonic vesicles located nearest the ovary showed signs of death and resorption earlier than those more distal to the ovary. Histological analysis allowed us to confirm that while the embryo implanted closest to cervix appeared healthy, the next one showed inflammatory cells in the yolk sac remains and the subsequent one showed an advanced process of embryonic resorption. More advanced stages of embryo resorption revealed hemorrhagic zones, fibrinoid and necrotic material, and inflammatory cells within the vesicles. All these characteristics clearly indicate that, concurrently with a diminished blood supply, immunological processes are involved in embryo resorption and deserve a further detailed analysis.

**The functionality of the placenta**

Optimal fetal growth depends on an efficient placental function. In fact, intrauterine embryonic growth restriction, fetal undernourishment and death may be related to placental insufficiency [35]. Unlike other mammals, including humans, where calcification of the placenta is a physiological event related to its aging and occurs at the end of pregnancy [36], placenta calcification in the vizcacha occurred early, from mid-gestation. Although placenta calcification is an indicator of loss of functionality, it does not seem to interfere with normal fetal development, since the most of the growth of the fetus that is gestated to term takes place in the presence of a calcified placenta. Early calcification of the placenta reinforces our previous hypothesis that the addition of secondary corpora lutea at mid-gestation helps to recover the decline of placental progesterone [9, 10].

The subplacenta is a structure with much more folding on the maternal side of the placenta. We showed here that the subplacenta from mid- and term-pregnant vizcachas undergoes apoptosis. Other studies have shown coincident observations in other hystricomorph rodents, in which part of the placenta loses connective tissue from mid-gestation, becomes more compact and produces degenerative changes [37, 38]. Likewise, we detected apoptosis in the basal decidua in early mid-pregnancy where the mineral deposits causing calcification were later localized. Apoptosis is a normal physiological process throughout pregnancy necessary to maintain immunosuppression in the pregnant uterus, protecting the fetus [39]. Apoptosis in the placenta of the fetuses that are gestated to term seems to be appropriately regulated since an alteration in this process would interfere with gestation and this was not evident. However, deregulation of the apoptotic process in anterior-implanted embryos needs a further examination in order to determine whether it directly influences or it is a by-product of the resorption process.

**Conclusions**

The analysis of arterial architecture and blood supply of the female genital tract in *L. maximus* provided evidence that blood stream, in the ascending circulation of the uterine horns through

the uterine artery, favors embryos implanted closest to the cervix. Therefore, a gradual nutritional deficiency is suspected in embryos as they implant closer to the ovary. Nutritional deficiency together with early calcification of the placenta suggests a role of both events in the embryo resorption process.

The presence of pseudosepta between the embryonic vesicles during pregnancy creates almost closed compartments that isolate the embryos from each other allowing the course of resorption in an almost independent way between them.

The presence of specialized endothelial venules and the detection of inflammatory cells in embryo vesicles undergoing resorption strongly suggest the participation of immunological processes during gestation that will require a detailed examination.

**Acknowledgments**

We acknowledge the Ministerio de Agroindustria, Dirección de Flora y Fauna, Province of Buenos Aires Government, for authorizing animal capture and the personnel of ECAS, Buenos Aires Province, for their help in trapping and handling the animals. We thank Dr. Juan Pablo Luaces for his technical assistance in vascular casting of the reproductive tract and Cátedra de Histología y Embriología, Facultad de CienciasVeterinarias, Universidad de Buenos Aires, for technical service in tissue processing.

**Competing interests**

The authors declared no potential conflicts of interest with respect to the research, authorship, and/or publication of this article.

**Author Contributions**

*Conceptualization:* MG and ADV; *formal analysis:* MG, JAC, PIFI and ADV; *funding acquisition:* SRF and ADV; *investigation:* MG, JAC, PIFI, FDL, MCG and SRF; *methodology:* MG, JAC, PIFI, FDL, MCG, SRF and ADV; *project administration:* MG and ADV; *resources:* MG, JAC, PIFI, FDL, MCG, SRF and ADV; *supervision:* ADV; *validation:* MG, JAC and PIFI; *visualization:* MG and PIFI; *writing - original draft preparation:* MG, PIFI, MCG and ADV; *writing - review & editing:* MG, JAC, PIFI, MCG and ADV. All authors have read and approved the final manuscript.

**Funding**

This research was funded by Agencia Nacional de Promoción Científica y Tecnológica, Argentina (PICT-2014-1281), and Fundación Científica Felipe Fiorellino, Universidad Maimónides, Buenos Aires, Argentina

## References

1. Llanos AC & Crespo JA. Ecología de la vizcacha (*Lagostomus maximus* Blainv.) en el nordeste de la provincia de Entre Ríos. Revista de Investigaciones Agrícolas. 1952;6:289-378.

2. Cabrera AL & Yepes J.Mamíferos Sudamericanos. 3rd edition. Buenos Aires: Ediar S.A.; 1960.

3. Cabrera AL. Catálogo de los mamíferos de América del Sur. Revista del Museo Argentino de Ciencias Naturales "Bernardino Rivadavia". Ciencias Zoológicas. 1961;4:309-732.

4. Jackson JE, Branch LC & Villareal D. *Lagostomus maximus*. Mammalian Species. 1996;543:1-6. doi 10.2307/3504168.

5. Weir BJ. The reproductive physiology of the plains viscacha, *Lagostomus maximus*. J Reprod Fert. 1971;25:355-363. doi 10.1530/jrf.0.0250355.

6. Roberts CM & Weir B. Implantation in the plains viscacha, *Lagostomus maximus*. J Reprod Fert. 1973;33:299-307. doi 10.1530/jrf.0.0330299.

7. Weir BJ. The reproductive organs of the female plains viscacha, *Lagostomus maximus*. J Reprod Fert. 1971;25:365-373. doi 10.1530/jrf.0.0250365.

8. Dorfman VB, Saucedo L, Di Giorgio NP, Inserra PIF, Fraunhoffer N, Leopardo NP, Halperin J, Lux-Lantos V & Vitullo AD. Variation in progesterone receptors and GnRH expression in the hypothalamus of the pregnant South American plains vizcacha, *Lagostomus maximus* (Mammalia, Rodentia). Biol Reprod. 2013;89:1-12. doi 10.1095/biolreprod.113.107995.

9. Jensen FC, Willis MA, Leopardo NP, Espinosa MB & Vitullo AD. The ovary of the gestating South American plains viscacha (*Lagostomus maximus*): suppressed apoptosis and corpora lutea persistence. Biol Reprod. 2008;79:240-246. doi 10.1095/biolreprod.107.065326.

10. Fraunhoffer N, Jensen F, Leopardo NP, Inserra PIF, Meilerman Abuelafia A, Dorfman VB & Vitullo AD. Hormonal behavior correlates with follicular recruitment at mid-gestation in the

South American plains vizcacha *Lagostomus maximus*. Gen Comp Endocrinol. 2017;250:162-174. doi 10.1016/j.ygcen.2017.06.010.

11. National Research Council. Committee for the Update of the Guide for the Care and Use of Laboratory Animals. USA: National Academy Press; 2011.

12. Jackson JE. Determinación de edad en la vizcacha (*Lagostomus maximus*) en base al peso del cristalino. Vida Silvestre. 1986;1:41-44.

13. Jensen F, Willis MA, Albamonte MS, Espinosa MB & Vitullo AD. Naturally suppressed apoptosis prevents follicular atresia and oocyte reserve decline in the adult ovary of *Lagostomus maximus* (Rodentia, Caviomorpha). Reproduction. 2006;132:301-308. doi 10.1530/rep.1.01054.

14. Leopardo NP, Jensen F, Willis MA, Espinosa MB & Vitullo AD. The developing ovary of the South American plains vizcacha, *Lagostomus maximus* (Mammalia, Rodentia): massive proliferation with no sign of apoptosis-mediated germ cell attrition. Reproduction. 2011;141:633-641. doi 10.1530/REP-10-0463.

15. Inserra PIF, Leopardo NP, Willis MA, Freysselinard AL & Vitullo AD. Quantification of healthy and atretic germ cells and follicles in the developing and post-natal ovary of the South American plains vizcacha, *Lagostomus maximus*: evidence of continuous rise of the germinal reserve. Reproduction. 2014;147:199-209. doi 10.1530/REP-13-0455.

16. Leopardo NP & Vitullo AD. Early embryonic development and spatiotemporal localization of mammalian primordial germ cell-associated proteins in the basal rodent *Lagostomus maximus*. Sci Rep. 2017;7:594. doi 10.1038/s41598-017-00723-6.

17. Giacchino M, Inserra PIF, Lange FD, Gariboldi MC, Ferrari SR & Vitullo AD. Endoscopy, histology and electron microscopy analysis of foetal membranes in pregnant South American plains vizcacha reveal unusual excrecences on the yolk sac. J Mol Histol. 2018;9:245-255. doi 10.1007/s10735-018-9764-5.

18. Leopardo NP, Inserra PIF & Vitullo AD. Germ cell (Ahmed RG eds.). Intech Open:Egipt; 2018. Chapter 5, Challenging the paradigms on the origin, specification and development of the female germ line in placental mammals. doi 10.5772/intechopen.71559.

19. Rezende LC, Kuckelhaus SAS, Galdos-Riveros AC, Ferreira JR & Miglino MA. Vascularization, morphology and histology of ovary in armadillo *Euphractus sexcinctus* (Linnaeus, 1758). Archivos de Medicina Veterinaria. 2013;45:191-196. doi 10.4067/S0301-732X2013000200011.

20. Gavrieli Y, Sherman Y & Ben-Sasson SA. Identification of programmed cell death *in situ* via specific labeling of nuclear DNA fragmentation. J Cell Biol. 1992;119(3):493-501. doi 10.1083/jcb.119.3.493.

21. Felipe AE. Un modelo descriptivo del sistema reproductor hembra del coipo (*Myocastor coypus*). II: los órganos tubulares. Revista Electrónica de Veterinaria. 2006;1-19.

22. Cevik-Demirkam A, Ozdemir V & Demirkan I. The ovarian and uterine arteries in the chinchilla (*Chinchilla lanigera*). J S Afr Vet Assoc. 2010;81:54-57. doi 10.4102/jsava.v81i1.97.

23. Weir BJ. Some observations on reproduction in the female Green acouchi, *Myoprocta pratti*. J Reprod Fert. 1971;24:193-201. doi 10.1530/jrf.0.0240193.

24. Weir BJ. Some observations on reproduction in the female agouti, *Dasyprocta aguti*. J Reprod Fert. 1971;24:203-211. doi 10.1530/jrf.0.0240203.

25. Flamini MA, Barbeito CG & Portiansky EL. A morphological, morphometric and histochemical study of the oviduct in pregnant and non-pregnant females of the plains viscacha (*Lagostomus maximus*). Acta Zoologica. 2014,95:186-195. doi 10.1111/azo.12018.

26. Flamini MA, Portiansky EL, Favaron PO, Martins DS, Ambrosio CE, Mess AM, Miglino MA & Barbeito CG. Chorioallantoic and yolk sac placentation in the plains viscacha (*Lagostomus maximus*). A caviomorph rodent with natural polyovulation. Placenta. 2011;32:963-968. doi 10.1016/j.placenta.2011.09.002.

27. Pradere JD, González FM, Ruiz EA & Correa A. Anatomía del útero y ovarios del capibara (*Hydrochoerus hydrochaeris*): irrigación arterial. Revista de la Facultad de Ciencias Veterinarias. 2006;47:25-32.

28. Egund M & Carter AM. Uterine and placental circulation in the guinea-pig: an angiographic study. J Reprod Fert. 1974;40:401-410. doi 10.1530/jrf.0.0400401.

29. Flamini MA, Barreto RSN, Matias GSS, Birbrair A, Harumi de Castro Sasahara T, Barbeito CG & Miglino MA. Key characteristics of the ovary and uterus for reproduction with particular reference to polyovulation in the plains viscacha (*Lagostomus maximus*, Chinchillidae). Theriogenology 2020;142:184-195. doi 10.1016/j.theriogenology.2019.09.043.

30. Céspedes R, Pradere J, Bermúdez V, Díaz T, Perozo E & Riera M. Irrigación arterial y venosa del útero y los ovarios de la perra (*Canis familiaris*) y su relación con la actividad

ovárica. Revista Científica de la Faculta de Ciencias Veterinarias de la Universidad del Zulia. 2006;16:353-363.

31. Abbas AK, Lichtman AHH & Pillai S. Cellular and molecular immunology. 9th edition. Elsevier; 2017. Chapter 3, Leukocyte circulation and migration into tissues. ISBN: 9780323523240.

32. Aguilar JJ, Cuervo-Arango J, Mouguelar H & Losinno L. Histological characteristics of the equine oviductal mucosa at different reproductive stages. J Equine Vet Sci.2012,32:99-105. doi 10.1016/j.jevs.2011.08.001.

33. Bosch P & Wright Jr RW. The oviductal sperm reservoir in domestic mammals. Archivos de MedicinaVeterinaria. 2005;37:95-105. doi 10.4067/S0301-732X2005000200002.

34. Steffl M, Schweiger M, Sugiyama T & Amselgruber W. Review of apoptotic and non-apoptotic events in non-ciliated cells of the mammalian oviduct. Ann Anat. 2008;190:46-52. doi 10.1016/j.aanat.2007.04.003.

35. Rossant J & Cross JC. Placental development: lessons from mouse mutants. Nat Rev Genet. 2001;2:538-548. doi 10.1038/35080570.

36. Sarkar M, Ingole IV, Ghosh SK, Bhakta A, Das RS & Tandale S. Calcification in placenta. J Anat Soc India. 2007;56:1-6.

37. Bonatelli M, Carter AM, Machado MRF, Oliveira MF, Lima MC & Miglino MA. Placentation in the paca (*Agouti paca* L.). Reprod Biol Endocrin. 2005;3:1-12. doi 10.1186/1477-7827-3-9.

38. Rodrigues RF, Carter AM, Ambrósio CE, Santos TC & Miglino MA. The subplacenta of the red-rumped agouti (*Dasyprocta leporine* L). Reprod Biol Endocrinol. 2006;4:1-31. doi 10.1186/1477-7827-4-31.

39. Jerzak M & Bischof P. Apoptosis in the first trimester human placenta: the role in maintaining immune privilege at the maternal-foetal interface and in the trophoblast remodelling. Eur J Obstet Gynecol Reprod Biol. 2002;2:142-146. doi 10.1016/S0301-2115(01)00431-6.

**Figure Legends**

**Figure 1. Anatomical sites of contrast solution administration for angiography or latex administration for vascular casting of the reproductive tract of female vizcacha.** Contrast solution was administrated in the abdominal aorta (A), the renal artery (B) or 1cm above the iliac artery bifurcation (C). Point C was also selected for the administration of latex for vascular casting.

**Figure 2. Angiographies of the reproductive tract of female vizcacha at different reproductive stages.** (A) Renal arteries visualized by administration of the contrast solution at the level of the abdominal aorta in a non-pregnant female. No evidence of the uterine circulation was observed. (B) Visualization of the uterine artery, and segmental arteries, by administration of the contrast solution 1cm above de iliac artery bifurcation; non-pregnant female. Blood circulation ascends from the vagina to the ovary. (C) Early-pregnant female showing bifurcation of abdominal aorta into iliac arteries and branching of the uterine artery. (D) Early-pregnant female showing the bifurcation of iliac arteries. (E) Placental circulation and uterine vasculature of the embryo implanted nearest the cervix at mid-pregnancy. (F) Placenta of the embryo implanted nearest the cervix absorbing all the contrast solution administered. R, right; L, left; E, embryonic vesicles; E1, embryo nearest the cervix.

**Figure 3. Vascular casting of the reproductive tract of the female vizcacha.** (A) General view of circulation of the reproductive tract by red latex casting in a non-pregnant female. (B) The uterine artery branches from the internal iliac artery and turns down the ureter to irrigate the uterine horn. (C) The uterine artery emits branches that irrigate the cervix and the uterine horn. (D) Circulation of the embryonic vesicle closest to the cervix in early-pregnancy. (E) Vascular remodeling in the uterine horn after embryonic resorption. The circulation of the uterine horn section proximal to the ovary was significantly reduced (arrow). (F) Embryo closest to the cervix, wrapped by extraembryonic membranes, separated by a septum from the rest of the embryonic resorption remains (arrow), at mid-pregnancy. (G) The ovarian artery emits branches to irrigate the ovary. (H) The distal end of the uterine arteries anastomose to the ovarian arteries (arrow). (1) bladder; (2) vagina; (3) uterine horn; (4) ureter; (5) uterine artery; (6) iliac artery; (7) segmental arteries; (8) pseudoseptum with circulation; (9) embryo closest to the cervix; (10) uterine horn with embryonic resorption; (11) fetus with its extraembryonic membranes; (12) ovary; (13) ovarian artery. Bar: A, 2cm; B, G and H, 1cm; C-E, 0.5 cm; F, 1.5 cm.

**Figure 4. Schematic representation of the vascular circulation of the genital tract of the female vizcacha.** The uterine artery, that irrigates each uterine horn, is a branch of the internal iliac arteries -a branch of the iliac artery which originates 1.5cm after the bifurcation of the abdominal aorta-. The uterine artery is located medially at the iliac crests, dorsal to the bladder and follows an ascending path through the broad ligament of the uterus. This artery emits

branches that irrigate the vagina, cervix, pseudosepta, uterine horns and oviduct. At the distal end, the uterine arteries anastomose to the ovarian arteries. E1: embryonic vesicle implanted nearest the cervix; E2: embryonic vesicle implanted anterior to E1.

**Figure 5. Histology of the uterine horn in pre-pubertal female vizcacha.** (A) Cross section of the uterine horn showing three layers: (1) endometrium, (2) myometrium and (3) perimetrium. B) Detail of the pseudostratified vaginal epithelium with mucosal cells (arrow). (C) Simple cylindrical epithelium of the uterine horn (arrow). The apical stroma presents more cellularity. Bar: A, 50µm; B and C, 20µm.

**Figure 6. Reproductive tract of non-pregnant female vizcacha.** (A) Macroscopic view of the genital tract showing longitudinal banding (arrow) of the uterine horn. (B) Longitudinal section of the vagina and the uterine sector closest to the cervix (arrows). Note the septum in the most cranial region. (C) Longitudinal section of the uterine horn with zigzag pattern (arrows) (D) Transition (circle) of the vaginal epithelium to uterine horn epithelium. (E) High epithelium venule (arrow). (F) Septum (arrow) that divides the oviduct lumen into different compartments. (G) Presence of peg cells in the ampulla (arrows). (H) Visualization of interspersed secretory and non-secretory cells by transmission electron microscopy. (I) Exfoliation of secretory cells from the apical zone of the oviduct toward the lumen. (1) ovary; (2) vagina; (3) vaginal septum; (4) cranial vagina; (5) vaginal epithelium; (6) uterine epithelium. Bar: A, 1cm; B, 0.25cm; C and F, 50µm; D and E, 10µm; G, 20µm; H and I, 1µm.

**Figure 7. Uterine horn of early-pregnant female vizcacha.** (A) Longitudinal section of one uterine horn of an early-pregnant vizcacha. The embryonic vesicle implanted nearest the cervix (E1) was the largest, while the rest were darker and smaller. (B) Longitudinal section of E1. (C) Pseudoseptum between the different embryonic vesicles, with a small aperture (arrow). (D) Necrotic embryonic vesicles were brownish red and were deformed by the aperture of the pseudoseptum (arrow). (E) Longitudinal section of a uterine horn where the embryonic vesicles were removed; the small aperture that communicates the adjacent vesicles (arrows) was evidenced. E2: second embryonic vesicle implanted from cervix; E3: third embryonic vesicle implanted from cervix; E4: fourth embryonic vesicle implanted from cervix; E5: fifth embryonic vesicle implanted from cervix. Bar: A-C and E, 0.5cm; D, 0.2cm.

**Figure 8. Histology of the uterine horn of the pregnant female vizcacha.** (A) Section of a recently implanted embryo corresponding to the uterine area closest to the cervix (E1). (B) E1 showing maternal lacunae (1) and yolk sac located in the middle (2). (C) E1 showing an organized trophoblast. (D) The second embryonic vesicle closest to the cervix (E2) shows disorganized trophoblast with a large number of fibroblasts. (E) E2 showing inflammatory

infiltrate and yolk sac remnants (arrow). (F) Pseudoseptum with uterine extensions toward the lumen, separating E2 and E3 embryo vesicles (arrow). (G-H) Folding of the uterine epithelium (arrows) and presence of embryonic necrotic remnants (E2 and E3). (I) Uterine flaps (arrow) that occupy part of the uterine lumen between the remains of the necrotic embryo. Bar: A-B and E, 20 µm; C, D and F-I, 50µm.

**Figure 9. Reproductive tract of the lactating female vizcacha.** (A) Multiple focuses of hemorrhage of the endometrium (arrow). (B) Presence of siderin-containing macrophages arranged in stipples (arrows). (C) Free iron granules (arrows). A-B, hematoxylin and eosin stain; C, Prussian blue stain. Bar: 20µm.

**Figure 10. Calcification and apoptosis in the placenta of the vizcacha.** (A, B) Mid-gestation placenta of the embryonic vesicle implanted closest to the cervix (E1) showed calcium deposits in the basal decidua. (C) In mid-pregnant vizcachas, apoptotic cells were detected in the subplacenta and the basal decidua by TUNEL reaction. (D) The term-pregnant placenta showed apoptotic cells only in the subplacenta. Bar: 50µm.

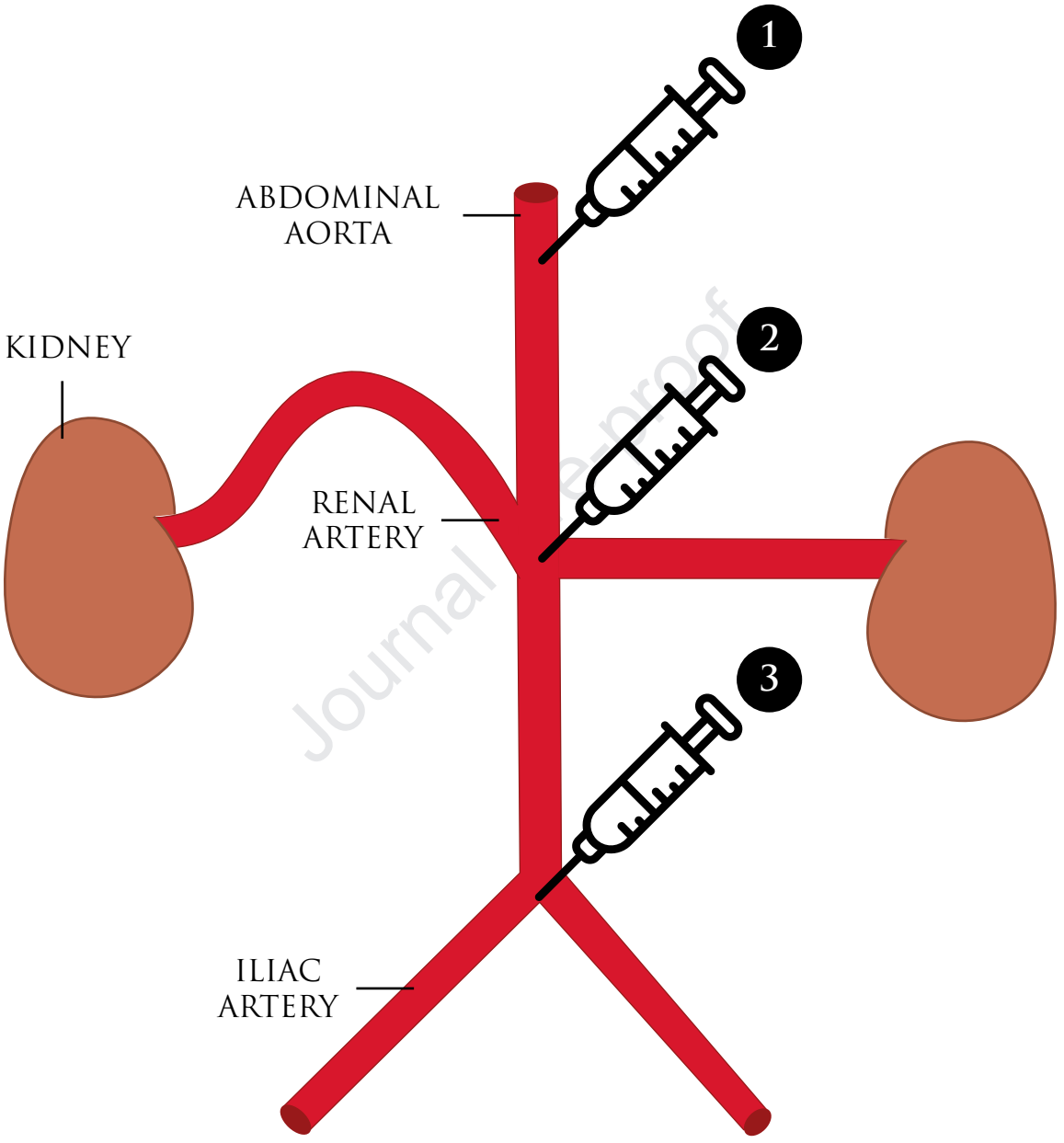

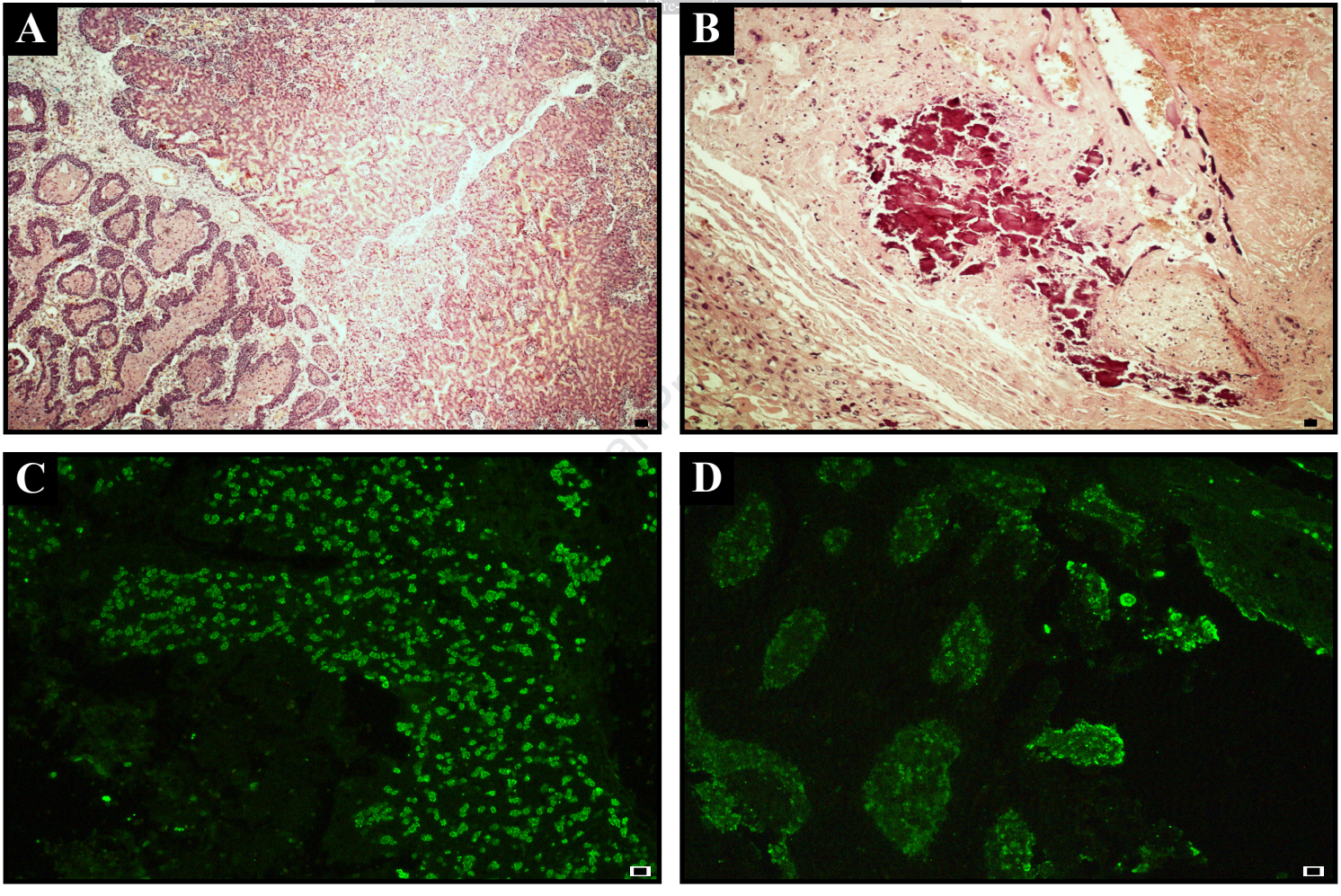
A
B
C
D

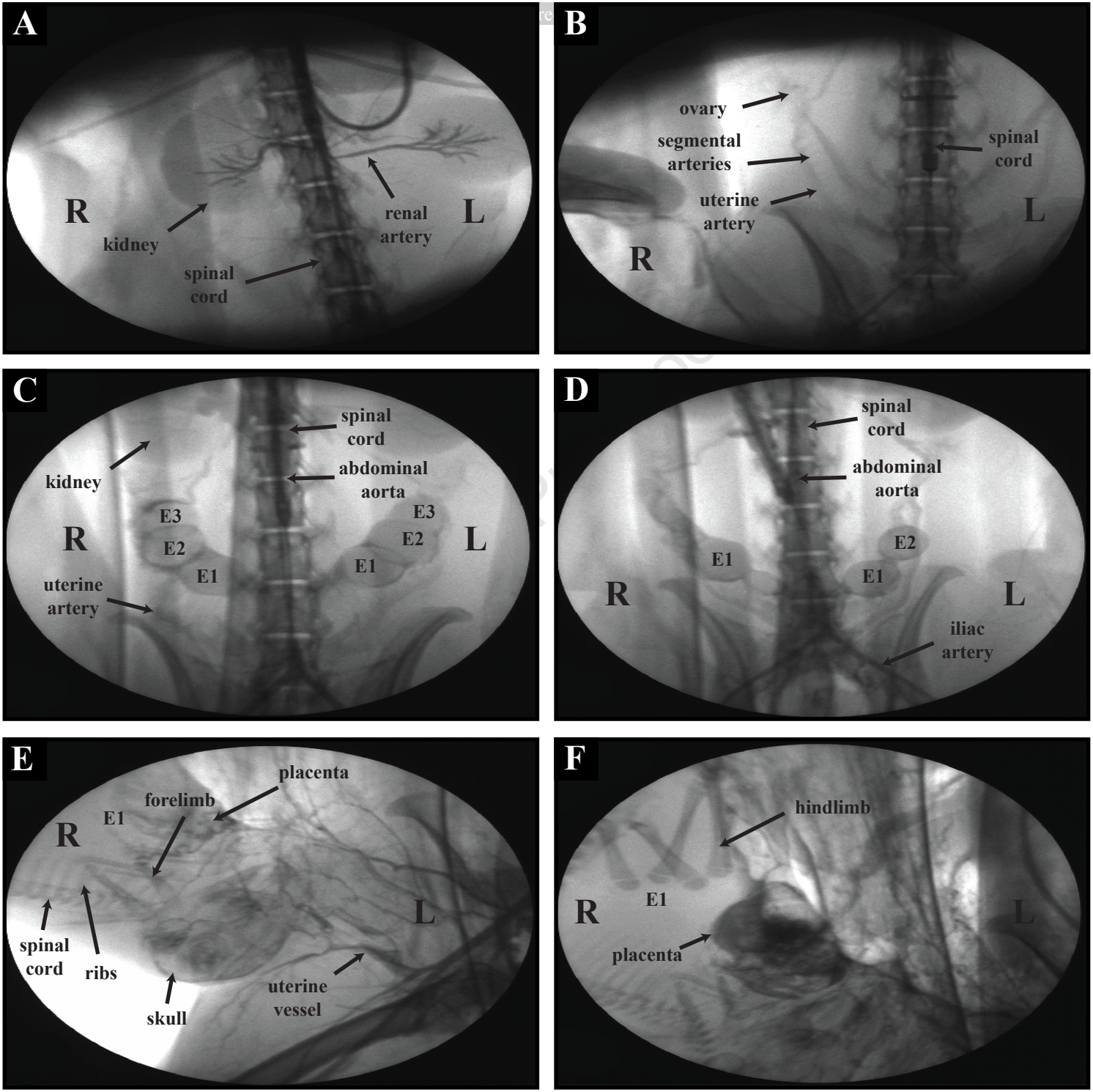
A
R
kidney
spinal cord
renal artery
L
B
ovary
segmental arteries
uterine artery
spinal cord
L
R
C
kidney
spinal cord
abdominal aorta
E3
E2
E1
R
E3
E2
E1
L
uterine artery
D
spinal cord
abdominal aorta
E2
E1
E1
R
L
iliac artery
E
placenta
forelimb
E1
R
L
spinal cord
ribs
skull
uterine vessel
F
hindlimb
R
E1
L
placenta

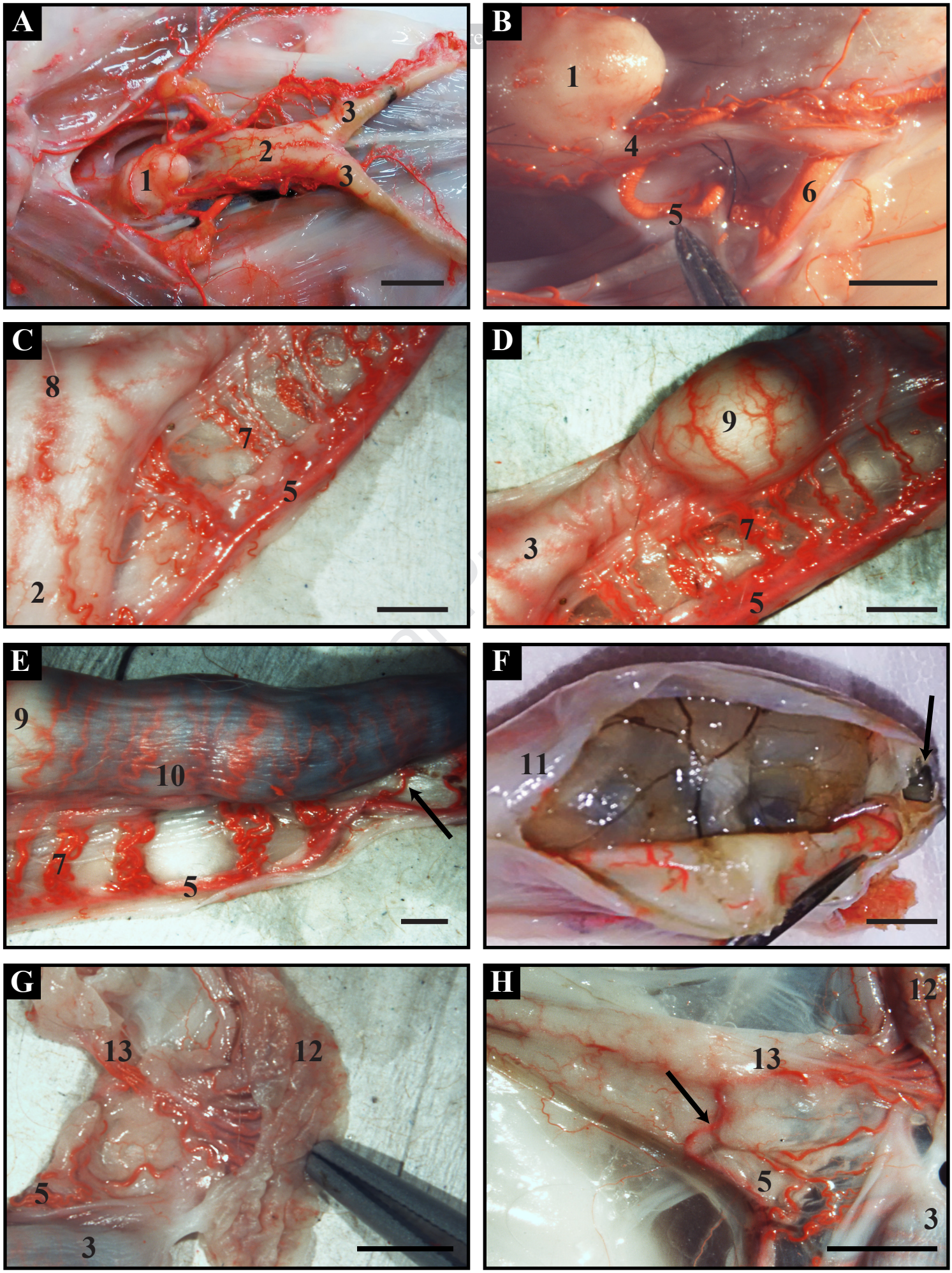
A
1
2
3
3
B
1
4
5
6
C
8
7
5
2
D
9
7
3
5
E
9
10
7
5
F
11
G
13
12
5
3
H
12
13
5
3

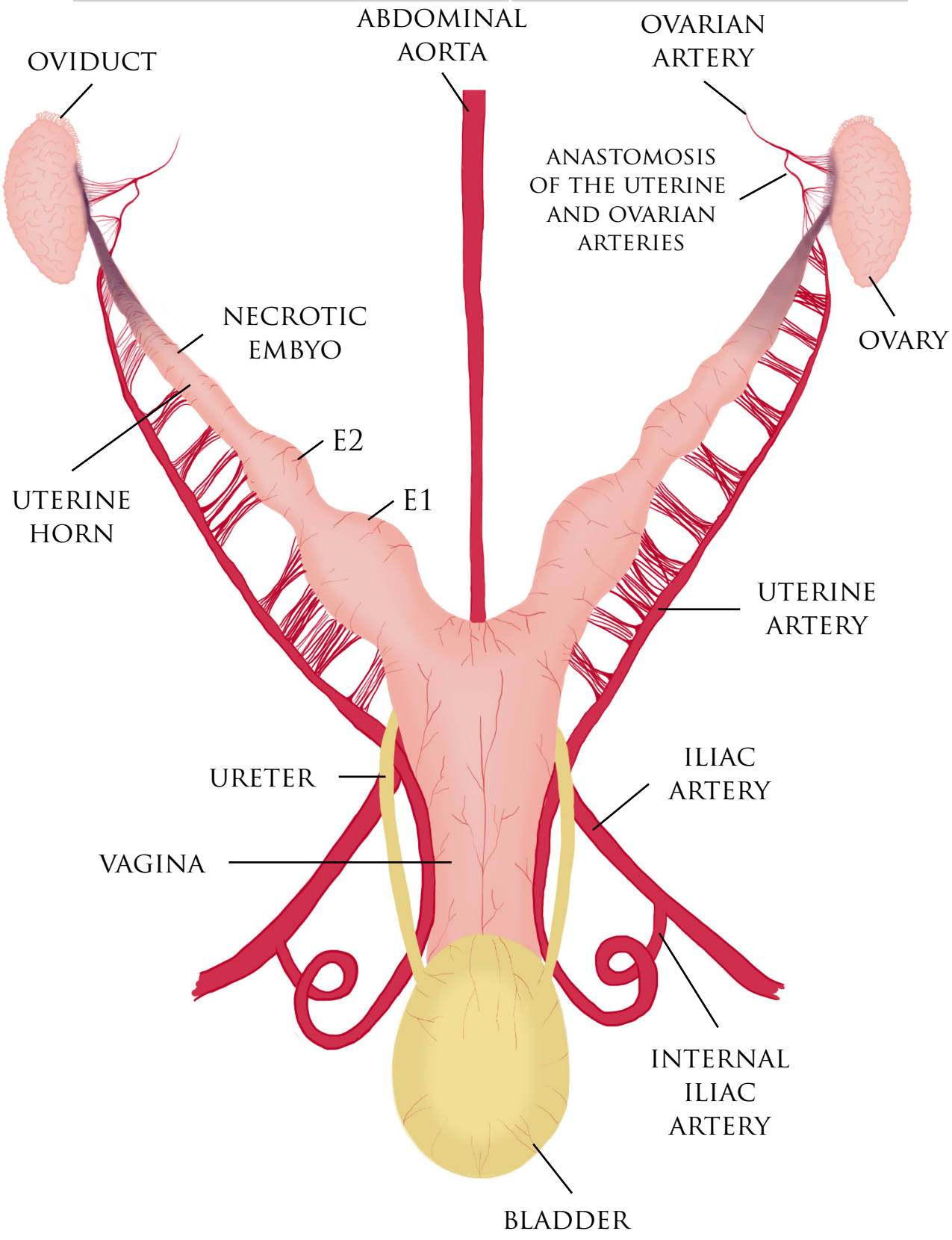

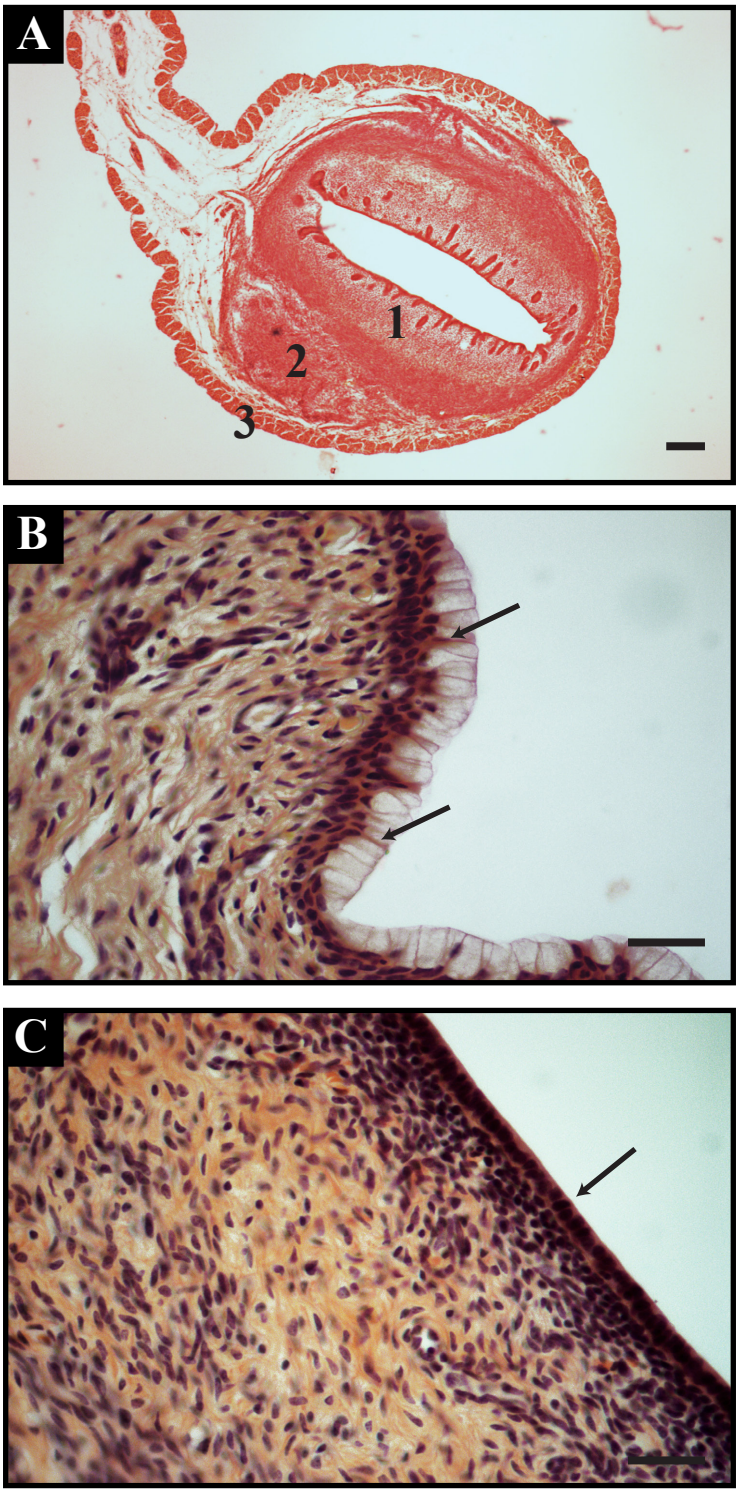
A
1
2
3
B
C

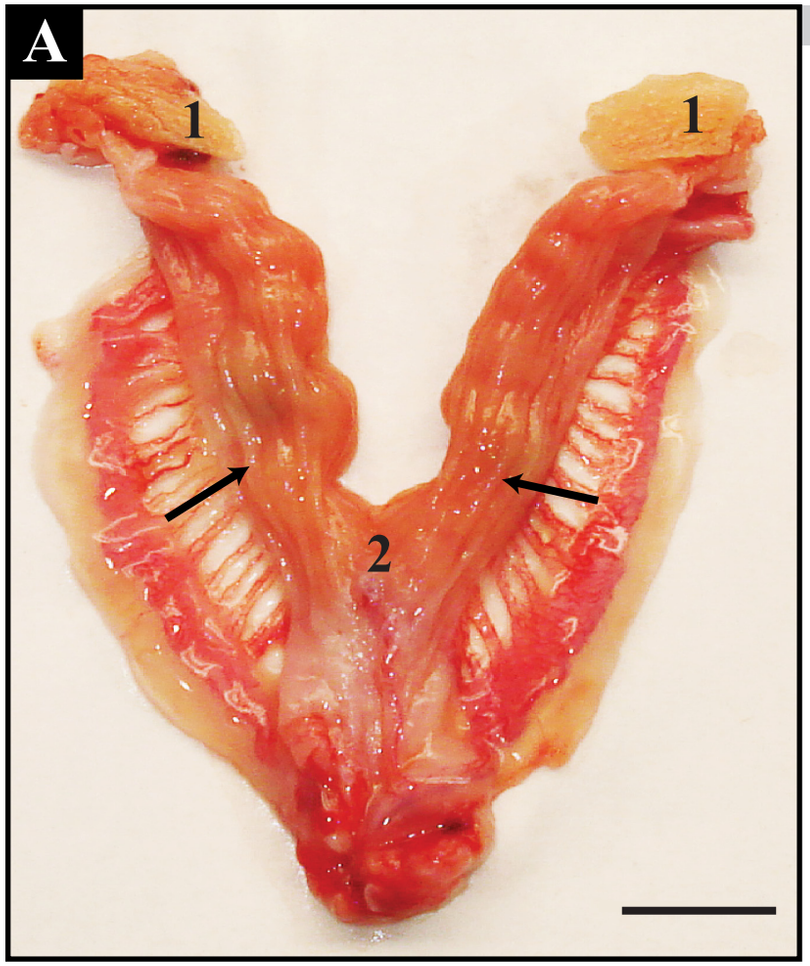
A
1
1
2


B
3
4


C

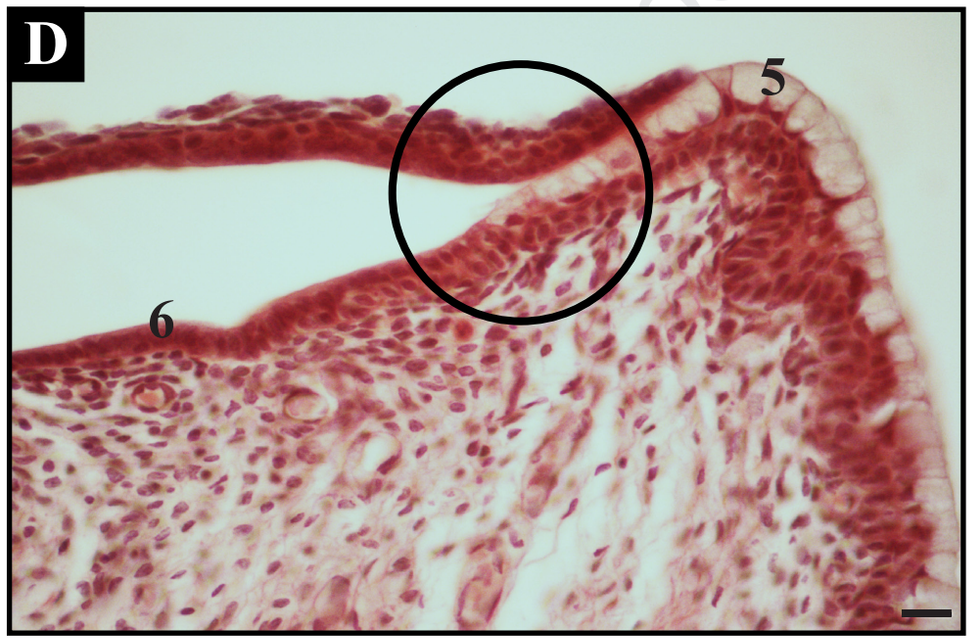
D
5
6

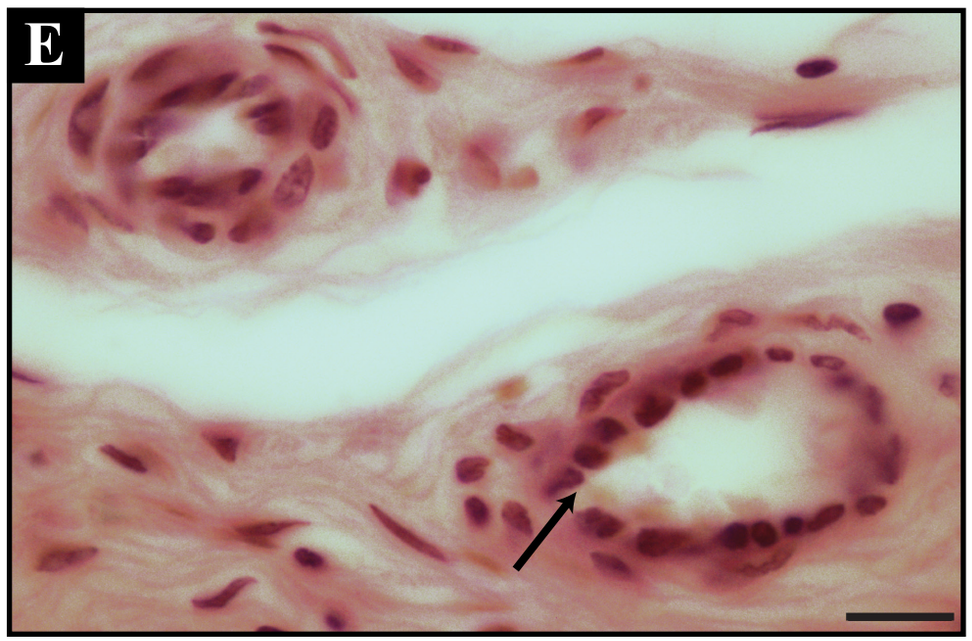
E

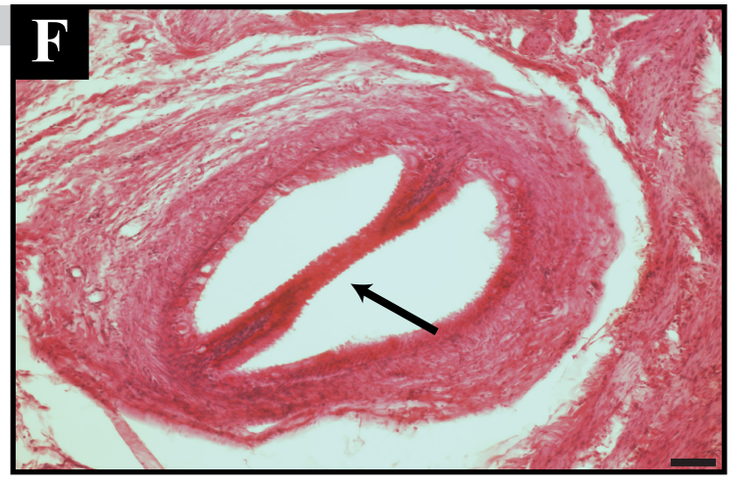
F

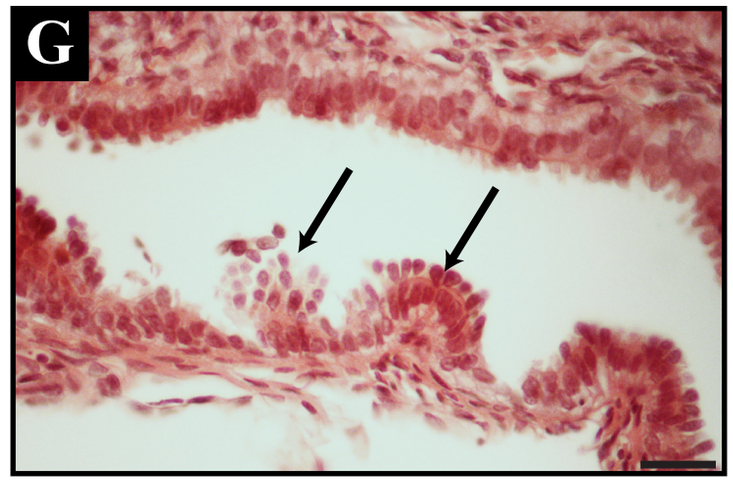
G

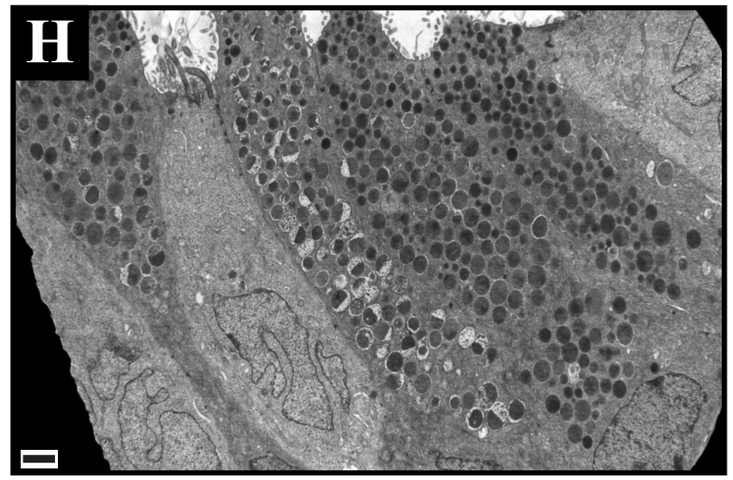
H

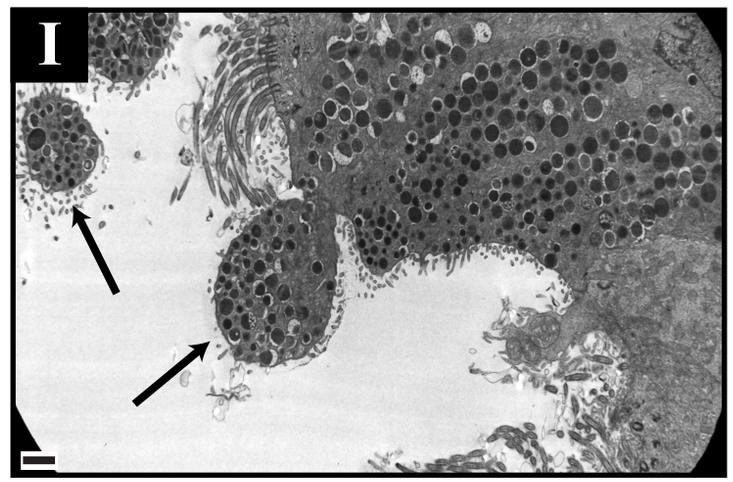
I

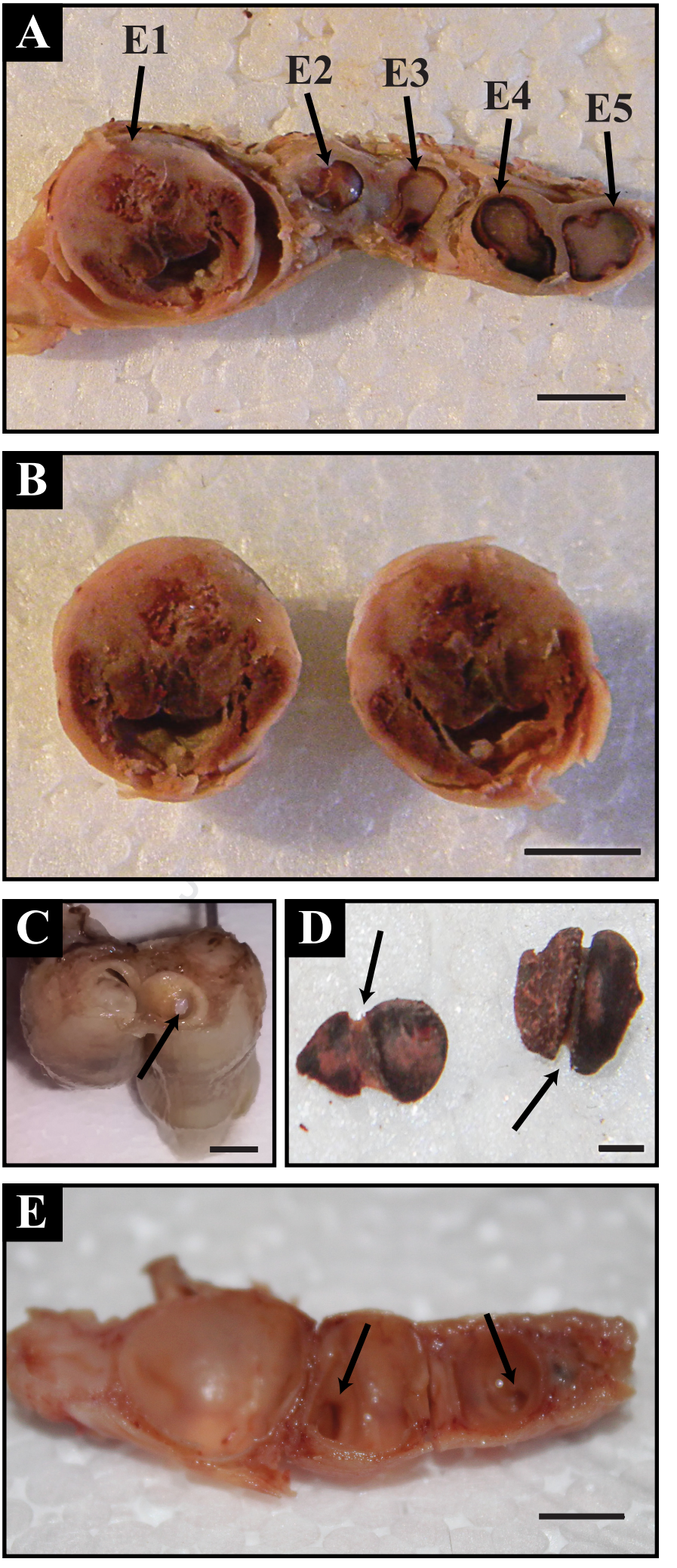
A
E1
E2
E3
E4
E5
B
C
D
E

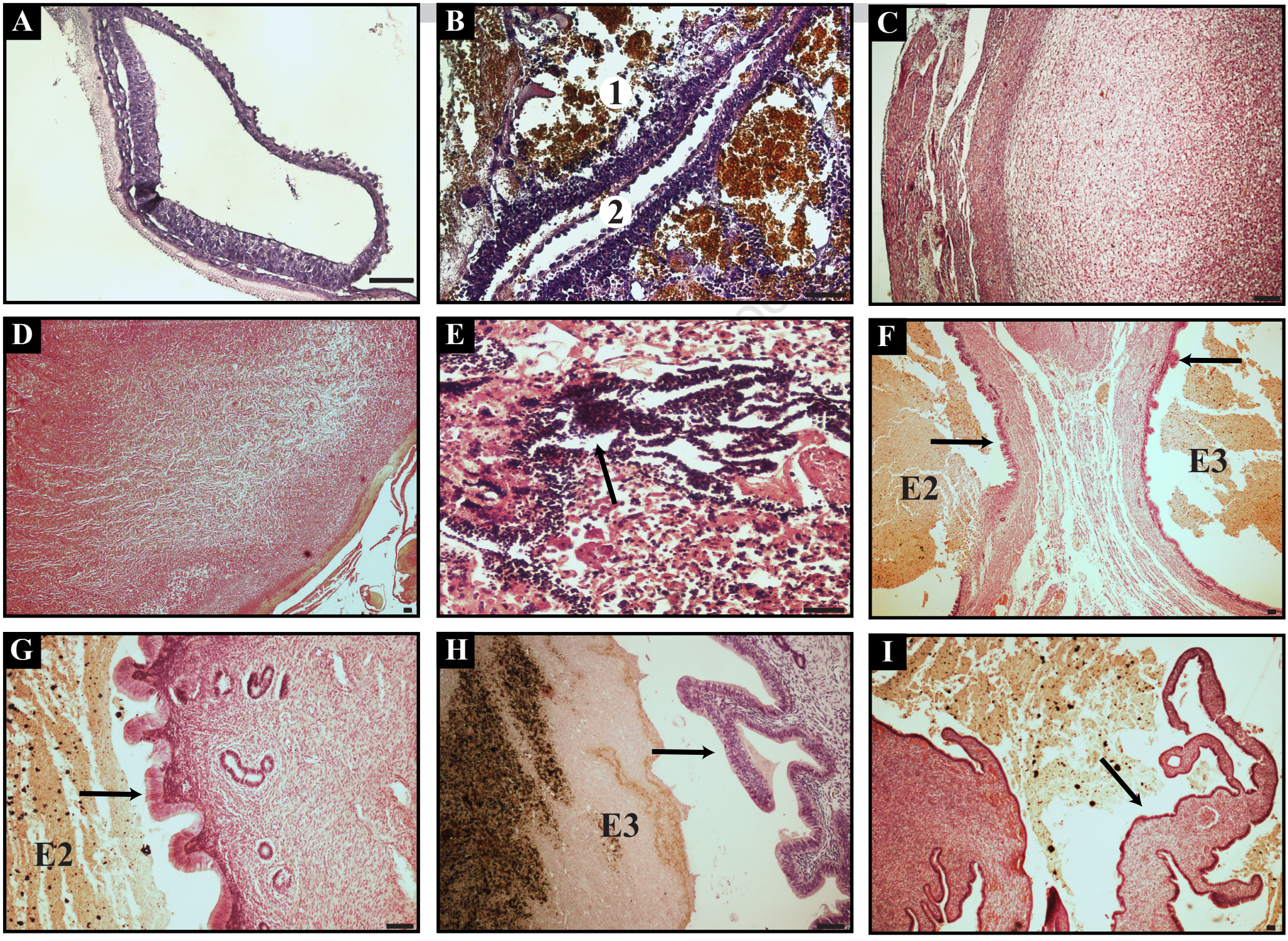
A
B
1
2
C
D
E
F
E2
E3
G
E2
H
E3
I

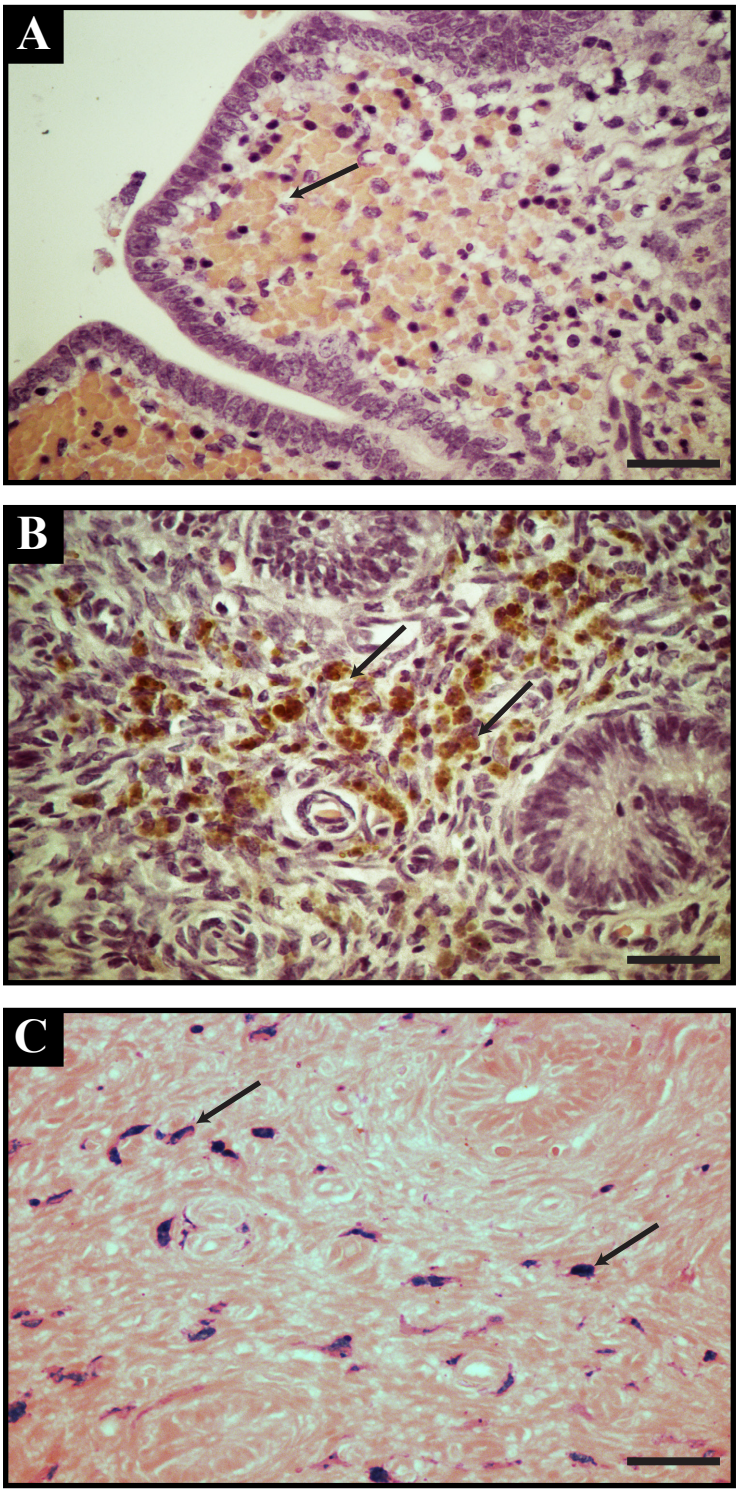
A
B
C

**Nutritional deficiency and placenta calcification underlie constitutive, selective embryo loss in pregnant South American plains vizcacha, *Lagostomus maximus* (Rodentia, Caviomorpha)**

Mariela Giacchino, Juan A Claver, Pablo IF Inserra, Fernando D Lange, María C Gariboldi, Sergio R Ferraris & Alfredo D Vitullo

## Highlights

- Female vizcacha displays selective, constitutive partial embryo resorption
- All embryos from both uterine horns are resorbed, except those implanted nearest the cervix
- Placenta becomes calcified early at mid-gestation
- Embryo vesicles are separated from each other by pesudosepta creating closed, isolated enclosures between them
- Ascending irrigation of the uterine horns favors embryos implanted closest to the cervix
- Nutritional deficiency and dysfunctional placenta seem to be at the basis of the resorption process